



*Dedicated to Professor Bogdan C. Simionescu
on the occasion of his 65th anniversary*

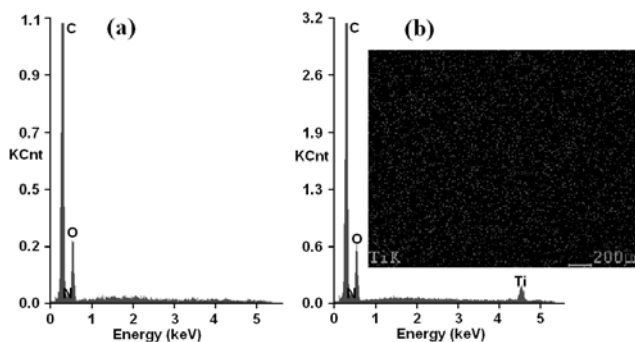
HYBRID POLYMER COMPOSITE COATINGS BASED ON PHOTOPOLYMERIZABLE PIPERAZINE DERIVATIVES MICROFILLED WITH TiO₂

Violeta MELINTE,* Tinca BURUIANĂ and Emil C. BURUIANĂ

“Petru Poni” Institute of Macromolecular Chemistry, 41 A Gr. Ghica Voda Alley, 700487, Iași, Roumania

Received September 28, 2012

In order to develop photopolymerized coating systems, it is crucial to use well-defined precursors. In this work, a low molecular weight piperazine/piperazinium dimethacrylate and an oligodimethacrylate having polytetrahydrofuran (M_w , 1000) as flexible spacer between the polymerizable end groups, were synthesized and used in the preparation of polymeric composites reinforced with silanized TiO₂ microparticles. Both monomers were characterized by spectral methods, and for a number of formulations containing about 30 wt. % piperazine/piperazinium dimethacrylates and Irgacure 819, other characteristics such as photoreactivity, surface and mechanical properties were investigated by specific measurements. Through the incorporation of TiO₂ microparticles (1-10 wt. %) before UV-curing of monomer mixtures the hydrophilicity of the composite surfaces and maximum tensile strength increased, whereas the elongation at break decreased. This study opens the possibility of making non-release antimicrobial coatings by depositing some appropriate compositions onto surfaces of various materials.



INTRODUCTION

In modern technology, the light-induced curing of acrylate/methacrylate multifunctional monomers and oligomers with the formation of highly crosslinked networks represents one of the most efficient pathways to quickly attain versatile materials widely applied in the fields of coatings, adhesives, hydrogels, paints, a.s.o.¹⁻³ The main advantages of this approach consist in the rapid

photopolymerization of the monomers upon exposure to UV light at room temperature in the absence of volatile solvents, into an environmentally friendly manner, allowing thus the formation of polymer networks through a fast transformation of the liquid monomers/oligomers into thin films, with novel and tunable physical, chemical and mechanical properties.⁴ Furthermore, the incorporation of inorganic micro/nanoparticles (e. g. clay, silica, hydroxyapatite, metals and metal oxides)

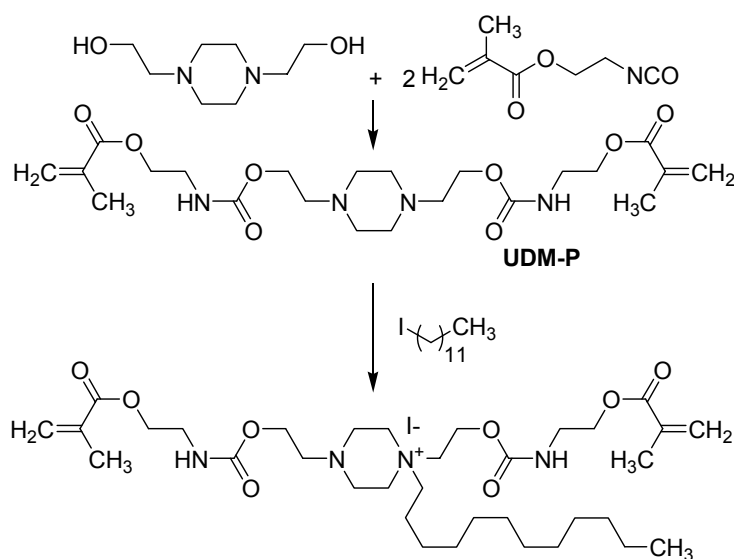
* Corresponding author: viomel@icmpp.ro

inside the organic photopolymerizable matrixes led to micro/nanofilled materials with different physico-chemical properties, such as flexibility, hardness, thermal/chemical stability or optical characteristics.⁵⁻⁷ In this context, many studies were performed on systems containing TiO₂ filler, taking into consideration its good physical and chemical properties, the large availability, potential antifouling and photobiocide properties as well as its photocatalytic activity.⁸⁻¹¹ Frequently, the titanium-containing hybrid materials have been prepared via the sol-gel method combined with a photopolymerization process,^{8,12} as well as by physical mixing of titanium oxide micro/nanoparticles and organic partners,^{9,13} depending on the targeted applicability field. In the second case, in order to improve the spreading rate of inorganic particles within the organic coatings and to attain an enhanced compatibility between TiO₂ filler and host polymeric materials, the use of organic modifiers for the filler particles is more suitable.^{14,15} Generally, the chemical modification of inorganic fillers is accomplished by means of trialkoxysilanes bearing photopolymerizable double bonds that render the surface of the filler more hydrophobic due to their ability to undergo hydrolysis and condensation reactions involving the hydroxyl groups present on the filler surface. Additionally, the existence of double bonds in such organic-inorganic monomers can improve the chemical interaction between the polymer chains and filler micro/nanoparticles avoiding their agglomeration.^{14,16}

The aim of this article is to extend our research focused on the hybrid composites containing a low quantity of noble metal nanoparticles using novel photopolymerizable urethane dimethacrylates that differ through functionalities, structure and chemical composition.¹⁷⁻¹⁹ Upon changing the monomer structure with other one bearing cationic functional group together with the nature of inorganic filler (TiO₂) new hybrid composites can be prepared via UV photopolymerization to investigate in a first part, some properties of such materials, for which the bioactivity of the antimicrobial monomers will be considered separately.

RESULTS AND DISCUSSION

Synthesis of the first photopolymerizable urethane dimethacrylate monomer containing piperazinium moieties assumed in the initial step the preparation of urethane dimethacrylate N,N-dimethacryloyloxyethyl-carbamoyloxyethyl piperazine (UDM-P) by the reaction of 1,4-piperazinediethanol with 2-isocyanatoethylmethacrylate, according to Scheme 1. Further, the amino groups present in the piperazine ring were partially quaternized with dodecyl iodide to afford the quaternary amine dimethacrylate (N,N-dimethacryloyloxyethyl-carbamoyloxyethyl dodecyl piperazinium iodide, UDM-QP), in which the degree of quaternization of the piperazine nitrogen was about 55%.



Scheme 1 – Reaction pathway for the obtaining of urethane dimethacrylate with piperazine/piperazinium groups (UDM-QP).

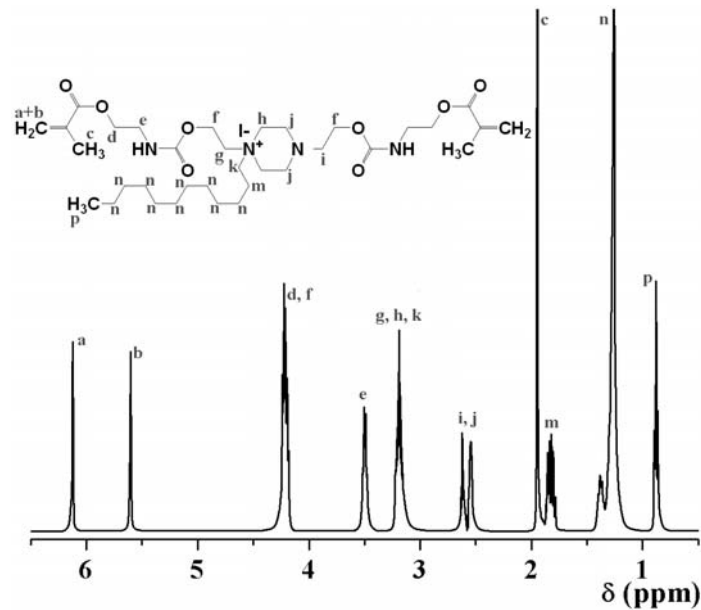


Fig. 1 – ^1H NMR spectrum of UDM-QP dimethacrylate in CDCl_3 .

The structure and purity of targeted products was verified through spectral methods, the ^1H NMR spectrum of UDM-QP dimethacrylate being illustrated in Fig. 1. Thus, the peak at 6.05 ppm corresponds to the unsaturated aliphatic protons in *trans*-position relative to the CH_3 unit, while the protons in *cis*-configuration can be observed at 5.52 ppm. Also, the methylene protons near to the ester-urethane units and the ester groups determined the appearance of the signal at 4.22 ppm, while the methylene protons linked to the urethane groups give the peak at 3.50 ppm. Other chemical shifts found in the spectral region are given by the methylene protons linked to the quaternary ammonium groups (3.19 ppm) and by those in the neighbourhood of nonquaternized amine groups (in the region 2.55-2.63 ppm), whilst the CH_3 protons from the methacrylic units appear at 1.95 ppm. The methylene protons in β position to quaternary structures can be observed at 1.82 ppm, whereas the other methylene protons coming from dodecane and the methyl protons from the same aliphatic chain were detected at 1.26 ppm and 0.88 ppm, respectively. The degree of quaternization of the piperazine nitrogen was determined from the integral ratio of protons i, j (2.66-2.63 ppm) vs. protons g, h, k (3.19 ppm).

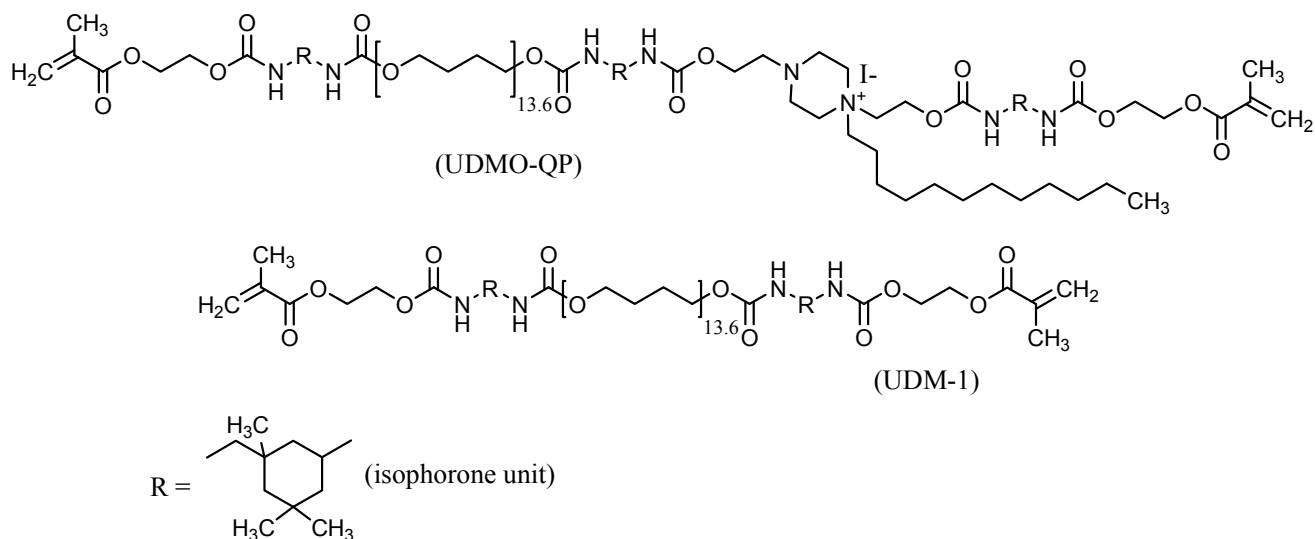
Another photopolymerizable urethane dimethacrylate employed in our study is of oligomer type, whose synthesis involved in the first preparative step a classical polyaddition reaction of polytetrahydrofuran ($M_w = 1000$) and 1,4-piperazinediethanol (in the molar ratio 1:1)

with isophorone diisocyanate to form a prepolymer with end isocyanate groups, which finally, is converted to macromer by a reaction with 2-hydroxyethyl methacrylate. Similarly, the cyclic amino groups from piperazine ring were quaternized with dodecyl iodide, an idealized structure of the resulting oligourethane dimethacrylate UDMO-QP (50% degree of quaternization) being depicted in Scheme 2. Again, the UDMO-QP was analyzed by ^1H NMR, its spectrum (unshown here) presenting the same resonances originating from the above mentioned protons and in addition, signals due to the PTHF protons, which are visible at 1.7 and 3.2 ppm.

A versatile approach frequently used to follow photopolymerization and photocrosslinking reactions occurred in the case of acrylic materials is based on FTIR spectroscopy, since the knowledge of curing degree for this type of derivatives is essential from the applicative point of view. Therefore, the vanishing of the double bond specific absorption bands from the FTIR spectra (located at about 1637 cm^{-1}) during UV irradiation was monitored, in order to evaluate the curing behaviour of two photopolymerizable acrylic mixtures. These mixtures contain 30 wt. % urethane dimethacrylate monomer/oligomer with piperazinium groups and 70 wt. % urethane dimethacrylate UDM-1 based on polytetrahydrofuran soft segments (structure given in Scheme 2, and whose preparation was reported²⁰) alongside 1 wt. % Irgacure 819 that act as photoinitiator. The choice of the co-monomer UDM-1 for copolymerization

reactions is motivated by the excellent film-forming quality with effect on the optical and mechanical properties. The graphical representation illustrated in Fig. 2 shows the gradual decay of the double bond absorption band for UDMO-QP/UDM-1 system with the irradiation time, so after 300 seconds of UV irradiation, the intensity of absorption peak is reduced to almost 80 %. Otherwise, the conversion plots presented in Fig. 2 b confirm the high conversion rates attained after 300 seconds of irradiation namely, of 67.5 % for the monomer system and of 79.8 % for the oligomer one. The differences appeared in the final conversion values can be attributed on one hand, to the viscosity variation between the monomer

mixtures used in our study (UDMO-QP is solid, while UDMO-QP oligomer is a viscous liquid), knowing that an increase of the photopolymerizable system viscosity will affect the macromolecular chains mobility and will decrease the double bonds conversion degree.²¹ Secondly, the diminution of the double bond concentration from 1.86 mmol g⁻¹ in monomer to 1.06 mmol g⁻¹ in UDMO-QP oligomer will generate in the first case a higher crosslinking degree which also will hinder the phototransformation of double bonds. As can be seen in Fig. 2 b, the conversion degree for UDMO-QP/UDM-1 in the first seconds of UV irradiation is higher than for the UDMO-QP/UDM-1 mixture.



Scheme 2 – Chemical structures of urethane dimethacrylate oligomers UDMO-QP and UDM-1.

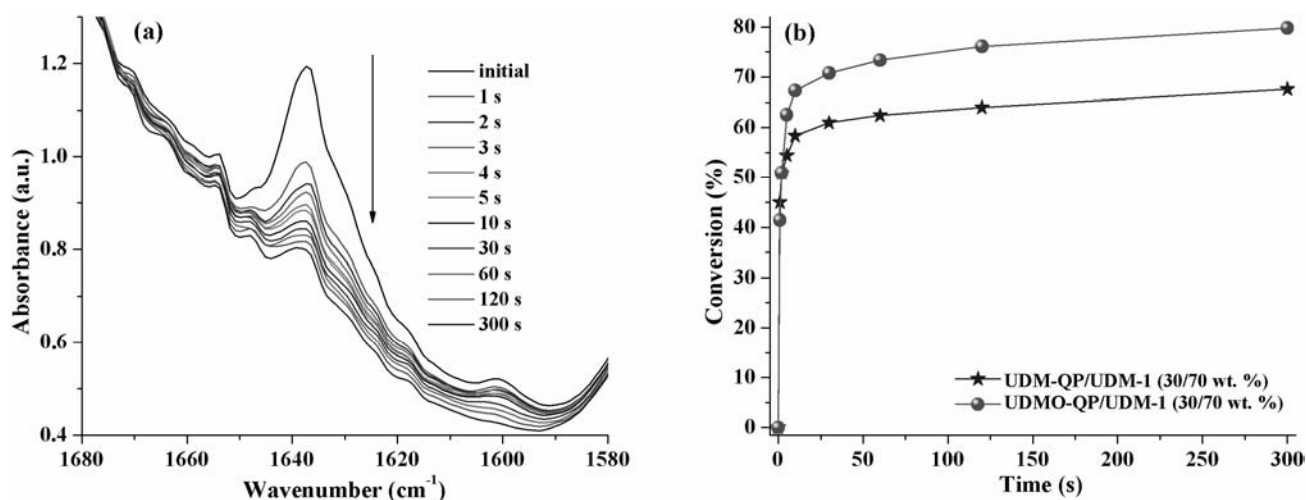


Fig. 2 – Modification of the double bond absorption band from the FTIR spectra during UV irradiation for UDMO-QP/UDM-1 mixture (a) and plots of double bond conversion versus irradiation time for both systems (b).

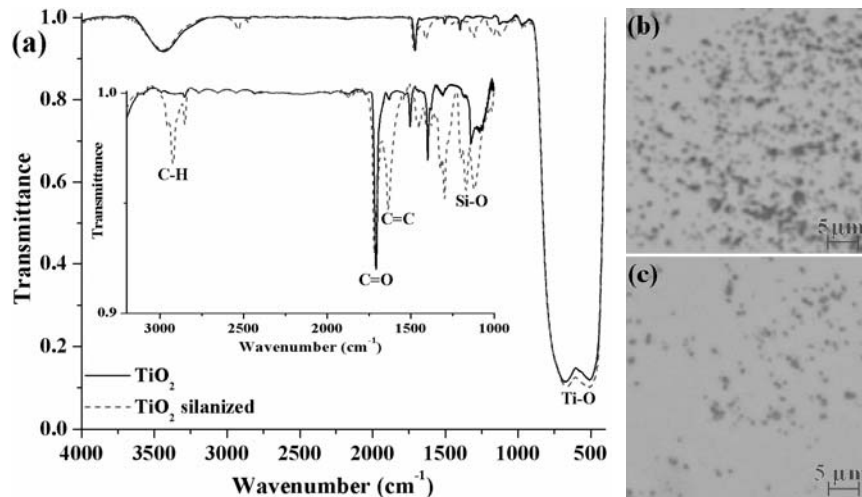


Fig. 3 – FTIR spectra of TiO_2 powder before and after silanization (a) and optical microscopy observation of TiO_2 powder before (b) and after (c) silanization.

In the recent literature, the concept of polymer-inorganic filler hybrid composites is one of the most popular areas of research, since the incorporation of low concentration of inorganic particles into the polymer matrix determines a significant improvement in physical properties of the resulting materials, especially, when the structural order within them can be controlled on nanometer/submicron scale. With this goal in mind, we prepared photopolymerized coatings, in which various amounts of titanium oxide were incorporated into the organic mixture before photopolymerization. Moreover, in order to enhance the adherence between the phases, the TiO_2 powder was silanized using 5 wt. % 3-(trimethoxysilyl)propyl methacrylate, a derivative that contain silane units and methacrylic photopolymerizable groups. Fig. 3, a shows the main differences in the FTIR spectra of titanium oxide powder before and after silanization. It can be observed the appearance of an absorption band at 2923 cm^{-1} attributable to the C-H vibrations, a band at 1636 cm^{-1} assigned to double bond vibration, while the Si-O linkages caused the development of characteristic stretching bands at 1170 and 1122 cm^{-1} . For further verifying the modification of TiO_2 particles with a hybrid monomer, their optical microscopy analysis was performed (Figure 3, b and c). Indeed, a better dispersion of the inorganic microparticles with dimensions between $0.5 - 1.0\text{ }\mu\text{m}$ become visible after silanization of TiO_2 particles.

The silanized TiO_2 particles were incorporated into the photopolymerizable mixtures in various proportions (between 1 and 10 wt. %), according to the formulations given in Table 1. Next, the hybrid mixtures were subjected to UV curing in the presence

of 1 wt. % Irgacure 819 photoinitiator to evaluate the properties of the cured systems according to the titanium content and the urethane dimethacrylate nature with piperazine/ piperazinium moiety.

First of all, the photopolymerization behaviour of monomer mixtures (already investigated by FTIR spectroscopy) with and without silanized TiO_2 was studied by means of photo-DSC, a largely used method to explore the photochemical reactions occurred in the case of photocrosslinkable systems. The major advantages of this method are conferred by the possibility of a fast evaluation of the most important parameters characterizing the curing kinetics of the photopolymerizable systems, namely the rate at the peak maximum ($R_{\text{max}}^{\text{p}}$) and the degree of double bond conversion (DC).

The polymerization rate profiles and the double bond conversion versus time for the considered photopolymerizable mixtures, assessed through photo-DSC measurements were displayed in Fig. 4. As can be noticed from Fig. 4, a (and from the photo-DSC data included in Table 2), the photoreactivity of the samples is relatively high, since the polymerization rate at the peak maximum is between 0.084 and 0.05 s^{-1} , and the time to reach the $R_{\text{max}}^{\text{p}}$ is very short (among 6.58 and 3.35 seconds). The highest polymerization rate was found for UDM-QP/UDM-1 mixture without inorganic filler (sample C1 with 0.084 s^{-1}), whilst the UDMO-QP/UDM-1 from C5 sample displays a lower polymerization rate (0.074 s^{-1}). Further, the polymerization rate decrease upon the incorporation of silanized TiO_2 filler and shifted to earlier times, suggesting that the inorganic particles hinder the mobility of growing radical chains formed during irradiation.

Table 1

Composition of some experimental hybrid composites, wettability trend (water contact angles) of the film surfaces and Young modulus values

Sample*	Piperazinium derivative	Loading content of silanized-TiO ₂ (wt. %)	Angle value (°)	Young modulus (MPa)
C1	UDM-QP	0	91.34	11.40
C2	UDM-QP	1	85.26	17.31
C3	UDM-QP	5	73.22	25.73
C4	UDM-QP	10	62.19	31.82
C5	UDMO-QP	0	91.07	7.16
C6	UDMO-QP	1	88.72	8.91
C7	UDMO-QP	5	77.73	12.07
C8	UDMO-QP	10	65.88	16.69

*each formulation contains 30 wt. % piperazinium derivative and 70 wt. % UDM-1, and is initiated with 1 wt. % Irigacure 819.

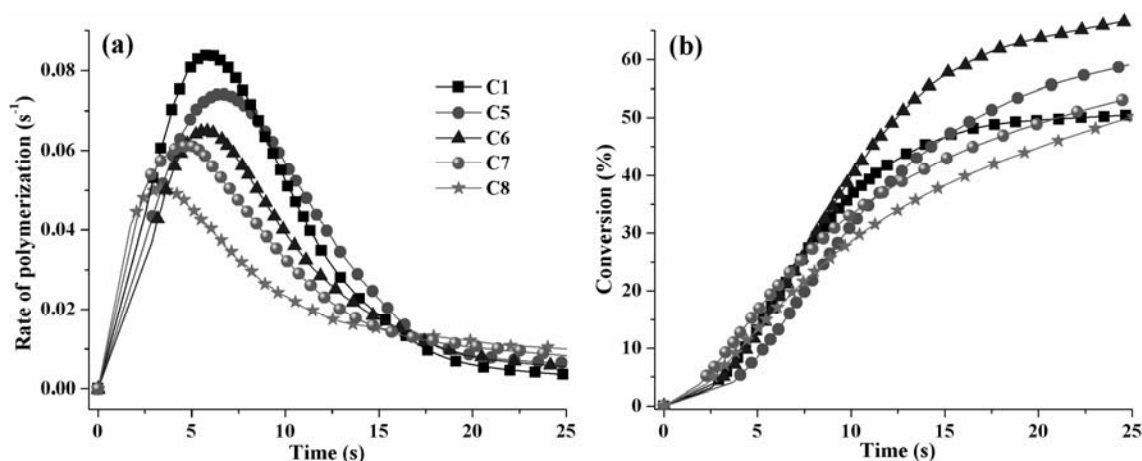


Fig. 4 – Photo-DSC rate profiles for the formulations C1, C5-C8 (a) and plots of their double bond conversion versus irradiation time (b).

Double bond conversion degree calculated after 3 minutes of UV irradiation (Table 2) varied between 62.73 % (C1) and 76.67 % (C6), and sustains the values determined through FTIR measurements for the samples without filler. It is important to note that the adding of 1 wt. % silanized TiO₂ favours an increase of the conversion degree from 73.93 % (C5) to 76.67 % (C6) as shown in Fig. 4, b. Obviously, there was an inverse relationship between the polymerization rate and the degree of conversion caused most probably by the microviscosity changes appeared during the polymerization process, as reported earlier.²² However, the inclusion of 5 or 10 wt. % TiO₂ particles inside the photopolymerizable organic matrixes led to a simultaneous decrease of polymerization rate and conversion degree for C7 and C8 systems. This behavior can be ascribed to the reducing in transparency induced by the

titanium oxide, where irradiation at longer wavelength is desired.²³ On the basis of this information, it can be concluded that C6 combination provide the best results in terms of double bond conversion versus silanized titanium dioxide amount.

The surface characteristics of photocrosslinked composite films were firstly investigated by means of water contact angle measurements (Table 1). Contact angle analysis furnishes data on the surface hydrophobicity/hydrophilicity and molecular mobility at an air/water/solid interface, given the importance of this feature on the applicability area of the resulting materials. According to the data included in Table 1, the measured contact angle for the C1-C8 samples varied between 91.34° and 62.19°, showing that the incorporation of inorganic TiO₂ particles favour the increase in surfaces wettability, feature

remarked for many other systems containing TiO₂ particles,^{13,24} and attributed to a large number of hydroxyl units at the surface of the particles.

Complementary data regarding the surface properties of composite films were achieved through 2-D elemental X-ray dot mapping, carried out using an environmental scanning electron microscope with energy-dispersive X-ray detector. Thus, the EDX analysis spectrum for C1 photopolymerized film without TiO₂ particles (Figure 5, a) demonstrates the existence of C, O and N elements, while in the EDX spectrum of C4 hybrid composite film the formation of the most abundant titanium characteristic peak at 4.54 keV can be observed, confirming therefore the presence of TiO₂ uniformly distributed inside the photopolymerized matrix.

An important aspect characterizing the polymeric films for coating applications that is expected to be modified by the inclusion of silanized titanium oxide was the mechanical behavior. The tensile test experiments were

performed on the photocrosslinked matrixes without inorganic filler (C1 and C5) comparatively to the hybrid composite materials (C2, C3, C4, C6, C7 and C8), the obtained data being displayed in Fig. 6 and Table 1. As can be seen from the stress-strain curves illustrated in Fig. 6, the incorporation of an increased percent of titanium oxide filler into the photopolymerized films determined the decrease of elongation at break (from 65 % in C1 to 41.5 % in C4, and from 80 % in C5 to 62 % in C8, respectively) simultaneously with the increase in maximum tensile strength (from 3.7 MPa in C1 to 5.3 MPa in C4 and from 3.4 MPa in C5 to 4.5 MPa in C8, respectively), confirming thus the reinforcing effect exerted by the TiO₂ particles on the mechanical behavior of hybrid composite films. The same trend can be perceived in the Young modulus variation (Table 1), which show that the inclusion of inorganic filler leads to an increase of the strength and modulus of the materials concomitantly with a decrease in their elasticity.

Table 2

Photo-DSC data for monomer combinations with and without silanized TiO₂ filler

Formulation	t _{max} (s)	Polymerization rate R _{max} ^P (s ⁻¹)	DC* (%)	Δ (J/g)
C1	5.94	0.084	62.73	47.57
C5	6.58	0.074	73.93	46.36
C6	5.83	0.065	76.67	48.08
C7	4.84	0.061	72.32	45.35
C8	3.35	0.050	70.56	44.25

* after 3 min of irradiation

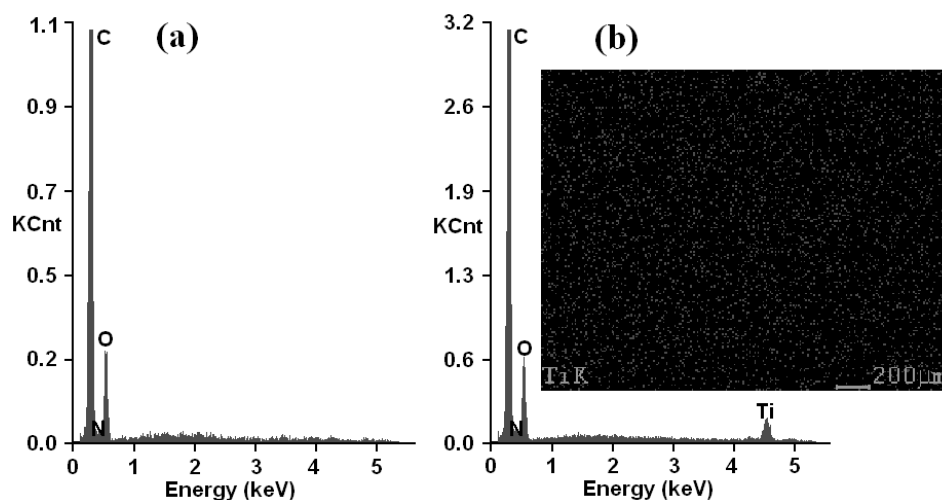


Fig. 5 – EDX analysis results for C1 film surface (a) and for C4 hybrid composite containing 10 wt. % TiO₂ filler together with titanium mapping image (b).

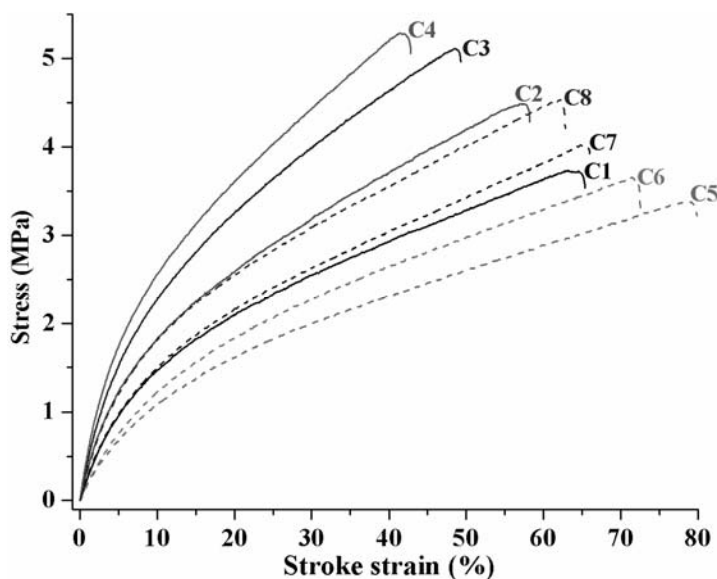


Fig. 6 – Stress-strain curves for photocrosslinked films with various percents of TiO₂ filler.

Moreover, comparing the two classes of composites, it can be observed that polymeric films containing urethane dimethacrylate monomer with piperazinium units (C1-C4) are more rigid than those with urethane dimethacrylate oligomer (C5-C8), behaviour that may be mainly attributed to the higher crosslinking density produced in the case of composite films enclosing monomer shorter counterparts. It is clear, however, that only a thorough understanding of such hybrid composites will allow for the design of nanocomposites for practical applications as permanent microbiocidal surfaces with non-leaching polymer antimicrobial coatings.

EXPERIMENTAL

Materials. Polytetrahydrofuran (PTHF, $M_n = 1000$) was purchased from BASF, 1,4-piperazinediethanol, 2-isocyanatoethylmethacrylate (IEMA), dodecyl iodide, isophorone diisocyanate, 2-hydroxyethyl methacrylate, 3-(trimethoxysilyl)propyl methacrylate (MPTS), phenyl-bis(2,4,6-trimethylbenzoyl) phosphine oxide (Irgacure 819) and titanium oxide (anatase) were purchased from Sigma Aldrich Chemical Co. and used without further purification.

Synthesis of *N,N*-dimethacryloyloxyethyl-carbamoyloxyethyl piperazine (UDM-P): 5 g (28.7 mmol) 1,4-piperazinediethanol were dissolved in 25 mL tetrahydrofuran and 8.27 mL (57.4 mmol) 2-isocyanatoethyl methacrylate were dropwise added, the mixture being stirred at 40 °C for 24 hours in the presence of dibutyltin dilaurate. After complete reaction, the UDM-P is collected by rotary evaporation under vacuum.

Synthesis of urethane dimethacrylate oligomer UDMO-P: 5 g (5 mmol) PTHF were degassed under vacuum for 2 hours and then 4.32 mL (20 mmol) IPDI were added, the mixture being stirred at 60 °C for 4 hours in the presence of catalytic amount of dibutyltin dilaurate. After that, 0.87 g (5 mmol) 1,4-

piperazinediethanol dissolved in 5 mL anhydrous tetrahydrofuran (THF) were added and the stirring continued for 5 hours. After a decrease of temperature at 40 °C, 2.44 mL (20 mmol) HEMA were added and the reaction continued for 10 hours. Finally, the UDMO-P is collected by rotary evaporation under vacuum.

Synthesis of quaternized monomer UDM-QP and oligomer UDMO-QP: 3 g of urethane dimethacrylate monomer/oligomer dissolved in THF were treated with equivalent amounts of dodecyl iodide calculated to attain maximum 75 % degree of quaternization, and were heated at 40 °C under stirring for 48 h. The resulting quaternized derivatives were collected by removing the solvent under vacuum and washing of the samples with diethyl ether.

Measurements. The structures of the urethane dimethacrylates were verified by ¹H NMR and FTIR spectroscopy using a Bruker 400 MHz spectrometer and a Bruker Vertex 70 spectrophotometer, respectively; the conversion degree was determined by FTIR, the kinetic parameters measured by photo-DSC, and the static water contact angle measurements and the mechanical tests were performed as previously described.¹⁹ The dimensions of TiO₂ particles were evaluated with an optical microscope (Leica DM 2500 M). EDX analysis of polymeric film surfaces were performed on an environmental scanning electron microscope QUANTA200 coupled with an energy dispersive X-ray spectroscope (ESEM/EDX). The dried samples were examined in low vacuum mode operating at 30kV using an LFD detector.

CONCLUSIONS

In this study two dimethacrylates with piperazine/piperazinium moieties differing by the presence or absence of flexible spacer were synthesized and used besides other urethane oligodimethacrylate (70 wt.%) taken as reactive co-monomer for the preparation of photopolymerized hybrid composites based on

polymer/TiO₂ microparticles (1-10 wt.%). Properties of the photocrosslinked composite coatings (photoreactivity, wettability, strength) can be correlated to the monomer structure, composition and the content of microparticles distributed in the organic matrix.

Acknowledgements: This work was financially supported by CNCSIS-UEFISCDI, project number PN-II-ID-PCE-2011-3-0164 (40/5.10.2011).

REFERENCES

1. R. Schwalm, *UV coatings: Basics, recent developments and new applications*, 1st edition, Elsevier: Amsterdam, The Netherlands, **2007**.
2. J. Kajtna and M. Krajnc, *Int. J. Adhes. Adhes.*, **2011**, *31*, 29-35.
3. T. Potta, C.J. Chun and S.C. Song, *Macromol. Rapid Commun.*, **2010**, *31*, 2133-2139.
4. Y. Wang, D.E. Betts, J.A. Finlay, L. Brewer, M.E. Callow, J.A. Callow, D.E. Wendt and J.M. DeSimone, *Macromolecules*, **2011**, *44*, 878-885.
5. Y.Y. Wang and T.E. Hsieh, *Chem. Mater.*, **2005**, *17*, 3331-3337.
6. H.-C. Chiang, C.-H. Liu and R. Tsiang, *J. Polym. Sci. Part A: Polym. Chem.*, **2008**, *46*, 8149-8158.
7. B.A. Rozenberg and R. Tenne, *Prog. Polym. Sci.*, **2008**, *33*, 40-112.
8. M. Sangermano, E. Amerio, A. Priola, A. Di Gianni and B. Voit, *J. Appl. Polym. Sci.*, **2006**, *102*, 4659-4664.
9. L.M. Hamming, R. Qiao, P.B. Messersmith and L.C. Brinson, *Comp. Sci. Technol.*, **2009**, *69*, 1880-1886.
10. N.P. Mellott, C. Durucan, C.G. Pantano and M. Guglielmi, *Thin Solid Films*, **2006**, *502*, 112-120.
11. A. Fujishima, T.N. Rao and D.A. Truk, *J. Photochem. Photobiol. C: Photochem. Rev.*, **2000**, *1*, 1-21.
12. M. Catauro, M.G. Raucci, D. De Marco and L. Ambrosio, *J. Biomed. Mater. Res.*, **2006**, *77A*, 340-350.
13. X. Zhao, W. Zhang, S. Chen, J. Zhang and X. Wang, *J. Polym. Res.*, **2012**, *19*, 9862.
14. A. Razmjou, J. Mansouri and V. Chen, *J. Membr. Sci.*, **2011**, *378*, 73-84.
15. A.L. Tolstov, V.F. Matyushov and D.O. Klymchuk, *Express Polym. Lett.*, **2008**, *2*, 449-459.
16. N. Al Dahoudi, J. Xi and G. Cao, *Electrochim. Acta*, **2012**, *59*, 32-38.
17. T. Buruiana, V. Melinte, F. Jitaru, E.C. Buruiana and L. Balan, *J. Polym. Sci. Part A: Polym. Chem.*, **2012**, *50*, 874-883.
18. V. Melinte, T. Buruiana, L. Balan and E.C. Buruiana, *React. Funct. Polym.*, **2012**, *72*, 252-259.
19. A. Chibac, V. Melinte, T. Buruiana, L. Balan and E.C. Buruiana, *Chem. Eng. J.*, **2012**, *200-202*, 577-588.
20. T. Buruiana, V. Melinte, A. Chibac, S. Matiu and L. Balan, *J. Biomater. Sci. Polym. Ed.*, **2012**, *223*, 955-972.
21. M.T. Lemon, M.S. Jones and J.W. Stansbury, *J. Biomed. Mater. Res.*, **2007**, *83A*, 734-746.
22. T. Buruiana, V. Melinte, F. Jitaru, H. Aldea and E.C. Buruiana, *J. Compos. Mater.*, **2012**, *46*, 371-382.
23. Y. Yagci, S. Jockusch and N.J. Turro, *Macromolecules*, **2010**, *43*, 6245-6260.
24. G. Wu, S. Gan, L. Cui and Y. Xu, *Appl. Surf. Sci.*, **2008**, *254*, 7080-7086.

